

Learning Topological Maps with Weak Local Odometric Information

Hagit Shatkay Leslie Pack Kaelbling
Computer Science Department, Box 1910
Brown University
Providence, RI 02912-1910
{hs,lpk} (Dcs.brown.edu)

Abstract

Topological maps provide a useful abstraction for robotic navigation and planning. Although stochastic maps can theoretically be learned using the Baum-Welch algorithm, without strong prior constraint on the structure of the model it is slow to converge, requires a great deal of data, and is often stuck in local minima. In this paper, we consider a special case of hidden Markov models for robot-navigation environments, in which states are associated with points in a metric configuration space. We assume that the robot has some odometric ability to measure relative transformations between its configurations. Such odometry is typically not precise enough to suffice for building a global map, but it does give valuable local information about relations between adjacent states. We present an extension of the Baum-Welch algorithm that takes advantage of this local odometric information, yielding faster convergence to better solutions with less data.

1 Introduction

Hidden Markov models (HMMs), as well as their extension to partially observable Markov decision processes (POMDPs) model a variety of nondeterministic dynamical systems as abstract probabilistic state-transition systems with discrete states, observations and possibly actions.¹ Such models have proven particularly useful as a basis for robot navigation in buildings, providing a sound method for localization and planning [Simmons and Koenig, 1995; Nourbakhsh *et al.*, 1995; Cassandra *et al.*, 1996]. Much previous work has required that the model be specified manually; this is a tedious process and it is often difficult to obtain correct probabilities.

An ultimate goal is for an agent to be able to learn such models automatically, both for robustness and in

¹ Actions are modeled by POMDPs but not by HMMs.

order to cope with new and changing environments. The Baum-Welch algorithm [Rabiner, 1989] is frequently used to learn HMMs. Since POMDPs are a simple extension of HMMs, they can, theoretically, be learned with a simple extension to the Baum-Welch algorithm. However, without strong prior constraint on the structure of the model, the Baum-Welch algorithm does not perform very well: it is slow to converge, requires a great deal of data, and is often stuck in local minima.

In this paper, we consider a special case of HMMs (extendable to POMDPs) for robot navigation, in which states are associated with points in a metric configuration space. We assume the robot has some odometric ability to measure relative transformations between its configurations. Such odometry is typically not precise enough to suffice for building a global map, but it does give valuable local information about relations between adjacent states. This information is readily available in most robots and is often ignored during the process of learning topological maps. We present an extension of the Baum-Welch algorithm that takes advantage of this local odometric information, yielding faster convergence to better solutions with less data.

2 Related Work

There has been a great deal of work on learning maps for mobile robotics and on learning stochastic models of dynamical systems in general. In this section, we focus on map learning for robots.

Sometimes it is necessary for a robot to know its location accurately in terms of metric coordinates; in such cases, metric maps are clearly the best choice. In many other environments, such as office buildings with corridors and rooms, or networks of roads, maps that simply specify the topology of important locations and their connections suffice. Such maps are typically less complex and support much more efficient planning than metric maps. Topological maps are built on lower-level abstractions that allow the robot to move along arcs (perhaps by wall- or road-following) and to recognize properties

of the locations; they are flexible in allowing a more general notion of state, possibly including information such as the robot's battery voltage or whether or not it is holding a bagel.

There are two typical strategies for deriving topological maps: one is to learn the topological map directly; the other is to first learn a geometric map, then to derive a topological map through some process of analysis.

A nice example of the second approach is provided by Thrun and Biicken [1996b; 1996a], who use occupancy-grid techniques to build the initial map. This strategy is appropriate when the primary cues for decomposition and abstraction of the map are geometric. However, in many cases, the nodes of a topological map are defined in terms of other sensory data (e.g. labels on a door). Learning a geometric map first also relies on the odometric abilities of a robot; if they are weak and the space large, it is very difficult to derive a consistent map.

We take the approach of learning the topological map directly, assuming that abstraction of the robot's perception and action abilities has already been done (we do it by hand, but see work of Pierce and Kuipers [1997] for an automatic method). Some approaches learn an underlying deterministic map of the world, independent of the noise in the robot's sensing and action processes. We prefer to learn a combined model of the world and the robot's interaction with the world; this allows robust planning that takes into account likelihood of error in sensing and action.

Kuipers and Byun [1991] provide a strategy for learning deterministic topological maps. It works well in domains in which most of the noise in the robot's perception and action is abstracted away, learning from single visits to nodes and traversals of arcs. It is unable to handle situations in which long strings of actions and observations are necessary to disambiguate the robot's location. Another set of learning algorithms, based on the theory of learning deterministic finite state automata, work in much noisier environments with much less global information. Basye, Dean, and Kaelbling [1995] provide algorithms for learning deterministic maps given fairly strong assumptions; these algorithms come with probabilistic correctness guarantees for learning in polynomial time with a polynomial amount of data.

Engelson and McDermott [1992] learn "diktiometric" maps (topological maps with metric relations between nodes) from experience. The uncertainty model they use is interval based rather than probabilistic, and the learned representation is deterministic. *Ad hoc* routines handle problems resulting from failures of the uncertainty representation.

The work most closely related to ours is by Koenig and Simmons [1996b; 1996a], who learn POMDP models (stochastic topological maps) of a robot hallway environ-

ment. They also recognize the impossibility of learning such a model without initial information; they solve the problem by using a human-provided topological map, together with further constraints on the shared structure of the model. A modified version of the Baum-Welch algorithm learns the parameters of the model. They also developed an incremental version of Baum-Welch that allows it to be used on-line in certain kinds of environments. Their models contain very weak metric information, representing hallways as chains of one-meter segments and allowing the learning algorithm to select the most probable chain length. This method is effective, but results in large models with size proportional to the hallways length.

We show that, by using odometric information directly, we can avoid the use of *a priori* models and still learn stochastic maps efficiently and effectively.

3 Models and Assumptions

In the following sections, we describe the model and algorithms used for learning an HMM, rather than a POMDP. Extension to POMDPs is technically straightforward but notationally more cumbersome.

The world is composed of a finite set of states. The states do not necessarily correspond directly to locations of the robot; they may include other state information, such as orientation or battery level. The dynamics of the world are described by state-transition distributions that specify the probability of making transitions from one state to the next. There is a finite set of observations that can be made in each state; the frequency of such observations is described by a probability distribution and depends only on the current state. In our model, observations are *multi-dimensional*, so an observation is a vector of values, each chosen from a finite domain. It is assumed that observation values are conditionally independent, given the state. Each state is assumed to be associated with a point in some metric space. Whenever a state transition is made, the robot records an *odometry vector*, which estimates the location of the current state relative to the previous state. It is assumed that the components of the odometry vector are corrupted with independent normal noise (extension to dependent noise is possible, and requires reestimation of the complete covariance matrix).

More formally, a model is a tuple $\lambda = \langle S, O, A, B, R, \pi \rangle$, where

- $S = \{s_1, \dots, s_N\}$ is a finite set of N states;
- $O = \prod_{i=1}^l O_i$ is a finite set of observation vectors of length l ; the i th element of an observation vector is chosen from the finite set O_i ;
- A is a stochastic transition matrix, with $A_{i,j} = Pr(q_{t+1} = s_j | q_t = s_i)$; $1 \leq i, j \leq N$; q_t is the state at

time t ;

- B is an array of l stochastic observation matrices, with $B_{i,j,o} = \Pr(V_i[i] = o | q_t = s_j)$; $1 \leq i \leq l$, $1 \leq j \leq N$, $o \in O_j$; V_i is the observation vector at time t ;
- R is a relation matrix, specifying for each pair of states, s_i and s_j , the mean and variance of the D -dimensional metric relation between them; $\mu(R_{i,j}[k])$ is the mean of the k th component of the relation between s_i and s_j and $\sigma^2(R_{i,j}[k])$, the variance; furthermore, R is *geometrically consistent*: for each component k , the relation $R^k(a, b) \stackrel{\text{def}}{=} \mu(R_{a,b}[k])$ must be a *directed metric*, satisfying the following properties for all states a, b , and c :
 - ◊ $R^k(a, a) = 0$;
 - ◊ $R^k(a, b) = -R^k(b, a)$ (*anti-symmetry*); and
 - ◊ $R^k(a, c) = R^k(a, b) + R^k(b, c)$ (*additivity*);
- π is a stochastic initial probability vector describing the distribution of the initial state; for simplicity it is assumed here to be $(1, 0, 0, \dots, 0)$, implying that the robot is always started in state s_0 .

A learning algorithm starts from an initial model λ_i and is given a sequence of experience E ; it returns a revised model λ , with the goal of maximizing $\Pr(E|\lambda)$. The experience sequence E is of length T ; each element is a pair (r_t, V_t) , where r_t is the observed relation between q_{t-1} and q_t and V_t is the observation vector at time t .

To extend the above model to a POMDP, *actions* need to be introduced into the model. Each possible action is associated with a separate set of three matrices A , B and R . In addition, each item in the experience sequence E contains the action which caused the transition and the observation associated with it. The algorithmic complexity of learning a POMDP compared with that of learning an HMM is within a factor proportional to the number of possible actions, which is usually much smaller than the number of states.

4 Algorithm

Our algorithm is a straightforward extension of Baum-Welch to deal with the relational information and the factored observation sets. The Baum-Welch algorithm is an expectation-maximization (EM) algorithm [Dempster et al., 1977]; it alternates between

- the *E-step* of computing the state-occupation probabilities γ at each time in the sequence given E and the current model λ , and
- the *M-step* of finding a new model λ that maximizes $\Pr(E|\lambda, \gamma)$.

An EM algorithm is guaranteed to provide monotonically increasing convergence of $\Pr(E|\lambda)$. Baum-Welch has been proven to be an EM algorithm; it has also been provably extended to real-valued observations [Liporace, 1982; Juang, 1985]. Our algorithm introduces an additional matrix, and enforces the first two geometric consistency constraints on the M-step, but like the standard Baum-Welch it is still guaranteed to converge to a local maximum of the likelihood function [Shatkay and Kaelbling, 1997]. The proof is along the lines of the one presented by Juang et al [1986] for the standard Baum-Welch algorithm, and is beyond the scope of this paper.

4.1 Computing State-Occupation Probabilities

Following Rabiner [1989], we first compute the forward (α) and backward (β) matrices. When all measurements are discrete, $\alpha_t(i)$ is the probability of observing E_0 through E_t and $q_t = s_i$, given λ ; and $\beta_t(i)$ is the probability of observing E_{t+1} through E_{T-1} given $q_t = s_i$ and λ . When some of the measurements are continuous (as is the case with R), these matrices contain probability density values rather than probabilities.

The forward procedure for calculating the α matrix is initialized with

$$\alpha_0(i) = \begin{cases} b_0^i & \text{if } \pi(i) = 1 \\ 0 & \text{otherwise} \end{cases},$$

and continued for $0 < t \leq T-1$ with

$$\alpha_t(j) = \sum_i \alpha_{t-1}(i) A_{i,j} f(r_t | R_{i,j}) b_t^j,$$

where $f(r_t | R_{i,j})$ is the density at point r_t according to the normal distribution represented by the means and variances in entry i, j of the relation matrix R , and b_t^j is the probability of observing vector v_t in state s_j ; that is, $b_t^j = \prod_{i=1}^l B_{i,j,v_t[i]}$.

The backward procedure for calculating the β matrix is initialized with

$$\beta_{T-1}(j) = 1,$$

and continued for $0 \leq t < T-1$ with

$$\beta_t(i) = \sum_j \beta_{t+1}(j) A_{i,j} f(r_{t+1} | R_{i,j}) b_{t+1}^j.$$

Given α and β , we now compute the state-occupation and state-transition probabilities (γ and ξ respectively). The state-occupation probabilities are computed as follows:

$$\begin{aligned} \gamma_t(i) &= \Pr(q_t = s_i | E, \lambda) = \frac{f(q_t = s_i, E | \lambda)}{f(E | \lambda)} \\ &= \frac{\alpha_t(i) \beta_t(i)}{\sum_{j=1}^N \alpha_t(j) \beta_t(j)}. \end{aligned}$$

Similarly, the state-transition probabilities are computed as:

$$\begin{aligned}\xi_t(i, j) &= \Pr(q_t = s_i, q_{t+1} = s_j | E, \lambda) \\ &= \frac{\alpha_t(i) A_{i,j} b_{i+1}^j f(r_{t+1} | R_{i,j}) \beta_{t+1}(j)}{\sum_{i=1}^N \sum_{j=1}^N \alpha_t(i) A_{i,j} b_{i+1}^j f(r_{t+1} | R_{i,j}) \beta_{t+1}(j)}.\end{aligned}$$

We note that the numerator and the denominator in the fractions are both density functions, but the quotient is a discrete probability function. These are essentially the same formulae appearing in [Rabiner, 1989], but taking into account the density of the relational observation.

4.2 Updating Model Parameters

In this phase of the algorithm, the goal is to find a new model, λ , that maximizes $P(E | \lambda, \gamma)$. Generally, this is done by simple maximum-likelihood estimation of the probability distributions in A and B by computing expected transition and observation frequencies. It is more difficult in our model, because we must also compute a new relation matrix, R , under the constraint that it remain geometrically consistent.

The A and B matrices can be straightforwardly re-estimated; $A_{i,j}$ is the expected number of transitions from s_i to s_j divided by the expected number of transitions from s_i :

$$A_{i,j} = \frac{\sum_{t=0}^{T-2} \xi_t(i, j)}{\sum_{t=0}^{T-2} \gamma_t(i)},$$

and $B_{i,j,o}$ is the expected number of times o is observed along the i th dimension when in s_j divided by the expected number of times of being in s_j :

$$B_{i,j,o} = \frac{\sum_{t=0}^{T-1} I(V_t[i] = o) \gamma_t(j)}{\sum_{t=0}^{T-1} \gamma_t(j)},$$

where $I(c)$ is an indicator function with value 1 if c is true and 0 otherwise.

If we were not going to enforce geometrical consistency, then the R matrix would be re-estimated by:

$$\begin{aligned}\mu(R_{i,j}[k]) &= \frac{\sum_{t=0}^{T-2} r_t[k] \xi_t(i, j)}{\sum_{t=0}^{T-2} \xi_t(i, j)} \\ \sigma^2(R_{i,j}[k]) &= \frac{\sum_{t=0}^{T-2} [r_t[k] - \mu(R_{i,j}[k])]^2 \xi_t(i, j)}{\sum_{t=0}^{T-2} \xi_t(i, j)}.\end{aligned}$$

In the current implementation, we enforce only two of the three constraints of geometrical consistency. Zero distances between states and themselves are trivially enforced. Anti-symmetry is enforced by using the data

from s_j to s_i as well as from s_i to s_j when reestimating $\mu(R_{i,j})$. Thus the actual reestimation formula for $\mu(R_{i,j})$ is:

$$\mu(R_{i,j}[k]) = \frac{\sum_{t=0}^{T-2} [r_t[k] \xi_t(i, j) - r_t[k] \xi_t(j, i)]}{\sum_{t=0}^{T-2} [\xi_t(i, j) + \xi_t(j, i)]}.$$

The additivity constraint is not currently enforced through the updates, although it is satisfied in the initial models, thus biasing the learned model towards satisfying it. We are exploring some relaxation techniques, based on spring systems, for enforcing the additivity constraint. The complexity of the algorithm per iteration is still $O(TN^2)$, like the standard Baum-Welch.

4.3 Finding an Initial Model

It is typical in instances of the Baum-Welch algorithm to simply initialize the model at random, perhaps trying multiple initial models to find different local likelihood maxima. We have tried random initial models, as well as starting from a more informed model, based on the odometry information. In both the random and informed initializations the initial R matrix satisfies all three properties of geometrical consistency.

To build an informed model, we begin by assigning global metric coordinates to each element in the sequence E . This is done by accumulating the observed relations between consecutive pairs of states. This data set (ignoring other observation information) is fed into a simple k-means clustering algorithm, yielding a clustering of the data into N clusters. The clusters are taken to be the states, and the observations associated with a given cluster are interpreted as having been generated in the associated state. We then compute γ and ξ values, with the γ values being 0 or 1, since we use a deterministic clustering algorithm (it might be beneficial to use a stochastic clustering algorithm, such as Autoclass [Cheeseman *et al.*, 1990]). The A , B , and R matrices are all estimated from γ and ξ as described in the previous section. Finally, an *ad hoc* process is used to adjust R to satisfy the additivity constraint.

5 Experiments

The goal of this work is to use odometry to improve the learning of topological models, while using fewer iterations and less data. We tested our algorithm in a simple robot-navigation world. Our experiments consist of running the algorithm both on data obtained from a simulated model and on data gathered by our mobile robot, Ramona, which is a modified RWI B21 robot. It has a cylindrical synchro-drive base, 24 ultrasonic sensors and 24 infrared sensors, situated evenly around its circumference. The infrared sensors are used mostly for short-range obstacle avoidance. The ultrasonic sensors

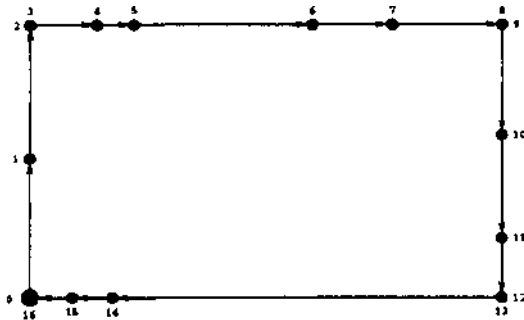


Figure 1: True map of the corridors Ramona traversed.

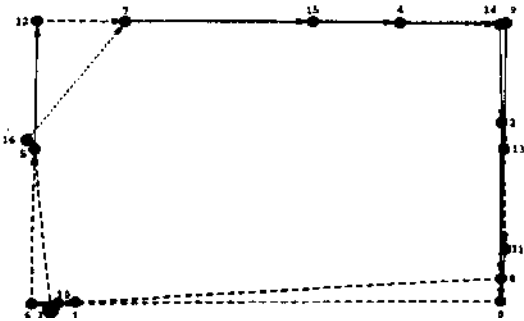


Figure 3: Learned map of the corridors Ramona traversed.

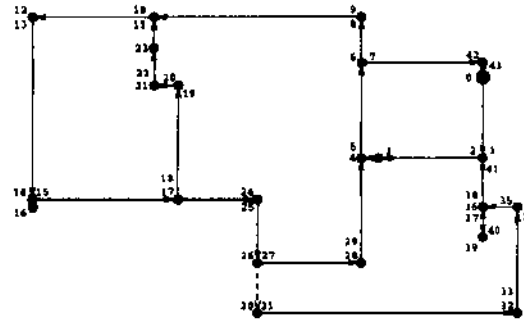


Figure 2: True map of simulated hallway environment.

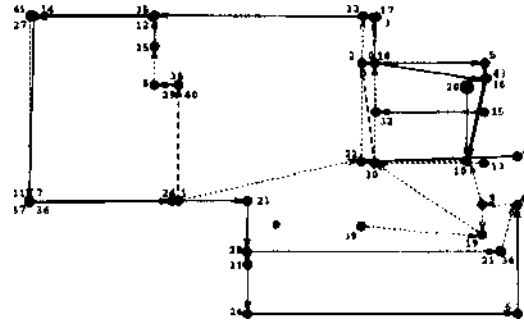


Figure 4: Learned map of the simulated hallway environment.

are longer ranged, and are used for obtaining (noisy) observations of the environment. The amount of data gathered by Ramona is used here as a proof of concept but is not sufficient for statistical analysis. For the latter, we use data obtained from the simulated model.

5.1 Robot Domain

The robot follows a prescribed path through the corridors in an office environment. Low-level software provides a level of abstraction that allows the robot to move through hallways from intersection to intersection and to turn ninety degrees to the left or right. At each intersection, ultrasonic data interpretation allows the robot to perceive, in each of the four cardinal directions, whether there is an open space, a door, a wall, or something unknown. The robot also identifies doors and openings that it passes along the corridors. Of course, both the action and perception routines are subject to error. Finally, the robot has encoders on its wheels that allow it to estimate its pose (position and orientation) with respect to its pose at the previous intersection. The path Ramona followed consists of 4 connected corridors in our building, which include 17 states, as shown in Figure 1.

In our simulation, we manually generated an HMM representing a prescribed path of the robot through the complete office environment, consisting of 44 states, and the associated transition, observation, and odometric distributions. Figure 2 shows the HMM corresponding to

the simulated hallway environment². Further interpretation of the figures is provided in the following section.

5.2 Evaluation Method

There are a number of different ways of evaluating the results of a model-learning algorithm. None is completely satisfactory, but they all give some insight into the utility of the results.

In this domain, there are transitions and observations that usually take place, and are therefore more likely than the others. Furthermore, the relational information gives us a rough estimate of the metric locations of the states. To get a *qualitative* sense of the plausibility of a learned model, we can extract an *essential* map from the learned model, consisting of the *states*, the *likely transitions* and the *metric measures* associated with them, and ask whether this map corresponds to the *essential* map underlying the true world.

Figures 1 and 2 are such essential versions of the true maps, while Figures 3 and 4 are essential versions of representative learned maps. Black dots represent the physical locations of states. Multiple states (depicted as numbers in the plot) associated with a single location typically correspond to different orientations of the robot at that location. The larger black circle represents the initial state. Arrows represent transitions that have probability 0.2 or higher. Solid arrows represent the most

²Observations and orientation are omitted for clarity.

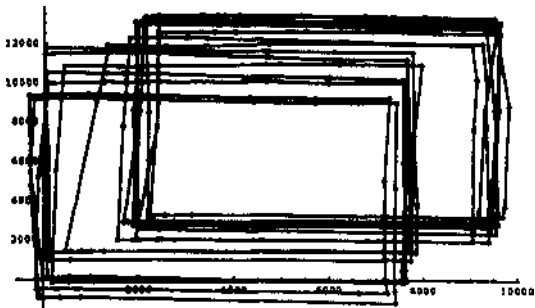


Figure 5: A data sequence gathered by Ramona.

likely transitions between the states, and dashed arrows represent the less likely ones³. Note that the length of the arrows is significant and represents the length of the corridors, drawn to scale.

More traditionally, in simulation experiments, the learned model is *quantitatively* compared to the actual model that generated the data. Each of the models induces a probability distribution on strings of observations; the asymmetric Kullback-Leibler divergence [Kullback and Leibler, 1951] between the two distributions is a measure of how good the learned model is with respect to the true model. Given a true probability distribution $P = \{p_1, \dots, p_n\}$ and a learned one $Q = \{q_1, \dots, q_n\}$, the KL divergence of Q with respect to P is:

$$D(P||Q) \stackrel{\text{def}}{=} \sum_{i=1}^n p_i \log_2 \frac{p_i}{q_i} .$$

We report our results in terms of a sampled version of the KL divergence, as described by Rabiner [1989]. It is based on generating sequences of sufficient length (5 sequences of 1000 observations in our case) according to the distribution induced by the true model, and comparing their likelihoods according to the learned model with the true model likelihoods. We ignore the odometry information when applying the KL measure, thus allowing comparison between models that are learned with and without odometry.

5.3 Results

We let Ramona go around the path depicted in Figure 1 and collect a sequence of about 300 observations. Figure 5 plots the sequence of metric coordinates obtained by accumulating consecutive odometric readings (as described in Section 4.3). We applied the learning algorithm to the data 40 times. 20 of these runs were started from an informed (cluster based) initial model and 20 started from a random initial model. (Note that there is non-determinism even when using informed initial models, since the clustering starts with random k-means, thus multiple runs give multiple results).

³Bold dashed arrows represent transitions that are *almost* as likely as the most likely.

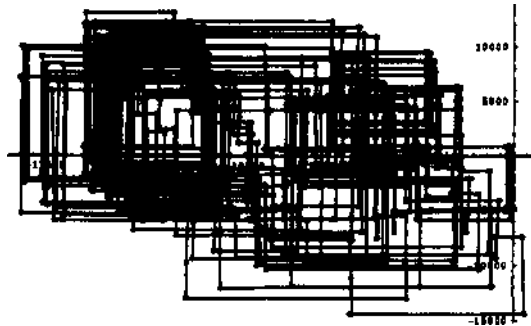


Figure 6: A data sequence generated by our simulator.

Figure 3 shows an essential representation of a typical learned map starting from an informed model. The geometry of the learned map strongly corresponds to that of the true map, and most of the states positions were learned correctly. Although the figure does not show it, the learned observation distributions at each state match well with the true observation distributions. When starting from an uninformed model, the results were not as satisfactory, which was predictable.

For obtaining statistically sufficient information, we generated 5 data sequences, each of length 1000, using Monte Carlo sampling from the model shown in Figure 2. One of these sequences is depicted in Figure 6. The figure demonstrates that the noise model used in the simulation is indeed compatible with the noise pattern associated with real robot data.

We used three different settings of the learning algorithm:

- starting from an informed (cluster based) initial model and using odometry information;
- starting from a random initial model and using odometry information;
- starting from a random initial model without using odometry information (standard Baum-Welch).

For each sequence and each of the three algorithmic settings we ran the algorithm repeatedly 5 times. In all the experiments, TV was set to be 44, which is the "correct" number of states; for generalization, it will be necessary to use cross-validation or regularization methods to select model complexity.

Figure 4 shows the essential version of one learned map (obtained from the sequence of Figure 6) for a representative run. We note that some of the states whose locations overlap in the true model (e.g. 8,9) become separated in the learned model (e.g. 33,17,3), due to noise in the odometry readings and observations. However, there is an obvious correspondence between groups of states in the learned and true models, and most of the transitions (as well as the observations, which are not shown) were learned correctly.

Seq. #	Informed		Random		No Odo	
	KL	Iter. #	KL	Iter. #	KL	Iter. #
1	2.347	93.40	3.797	110.00	10.129	201.80
2	2.338	84.00	2.630	82.00	11.400	213.80
3	2.672	85.80	3.086	160.00	11.683	195.40
4	3.185	85.20	3.632	114.20	11.810	224.00
5	4.154	116.20	3.877	102.40	12.258	166.80

Table 1: Average results of three learning settings with five training sequences.

Table 1 lists the KL divergence between the true and learned model, as well as the number of runs until convergence was reached, for each of the 5 sequences under each of the 3 learning settings, averaged over 5 runs per sequence. From the table it is clear that the KL divergence with respect to the true model for models learned using odometry, starting from either an informed or a random initial model, is about 4 *times smaller* than for models learned without odometry data. The standard deviation around the means was about 1.5 for all KL distances. To check the significance of our results we used the simple two-sample t-test. The models learned using odometric information have statistically significantly ($p < 0.005$) lower average KL divergence than the others.

In addition, the number of iterations required for convergence when learning using odometry information is roughly half that required when ignoring odometry information. Again, the t-test verifies the significance of this result.

The initial clustering strongly biases the outcome of learning; it is important to understand whether this bias is useful. When the entire model is initialized at random, the convergence time (measured in number of iterations) as well as the KL measure are somewhat higher on average, than when starting at an initial model based on clustering. The difference between the two starting points is not highly statistically significant since the clustering in many cases is not good. When the initial clustering is good, most of the work is already done and the EM algorithm quickly fills in the details. However, if the initial clustering is bad, it is often close to a poor local minimum and the algorithm is unable to adjust it well. It will be important to try more sophisticated clustering algorithms. It may be best to run the algorithm multiple times, some with initial clustering and some without, taking the model with the highest likelihood as the final result.

To examine the influence of the amount of data on the quality of the learned models, we took one of the 5 sequences (Seq. #1) and used its prefixes of length 100 to 1000 (the complete sequence), in increments of 100, as individual sequences. We ran each of the three algorithmic settings over each of the 10 prefix sequences, 10 times repeatedly. We then used the KL-divergence as described above to evaluate each of the resulting models

Seq. length	Informed		Random		No Odo	
	Mean KL	Std. Dev.	Mean KL	Std. Dev.	Mean KL	Std. Dev.
1000	2.097	0.71	3.016	1.24	10.139	1.90
800	1.808	0.28	2.954	1.75	13.319	1.26
600	2.353	1.14	2.369	1.36	14.642	1.62
400	2.953	0.60	2.801	1.69	22.714	4.69
300	3.998	1.53	3.892	3.60	$\rightarrow \infty$	NA
200	9.169	3.09	7.489	5.26	$\rightarrow \infty$	NA
100	$\rightarrow \infty$	NA	$\rightarrow \infty$	NA	$\rightarrow \infty$	NA

Table 2: Average results of three learning settings with 10 incrementally longer sequences .

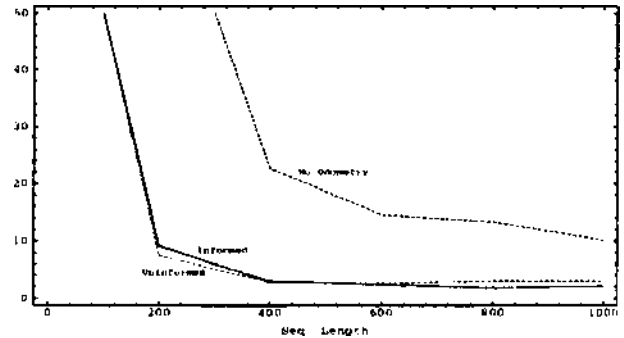


Figure 7: Average KL-divergence as a function of the sequence length.

with respect to the true model. For each prefix length we averaged the KL-divergence over the 10 runs.

Table 2 summarizes the results of this experiment. It lists the mean KL-divergence over the 10 runs for each of the prefixes, as well as the standard deviation around this mean. Entries with KL-divergence $\rightarrow \infty$ indicate that sequences generated by the true model were assigned negligible (-0) probability by the learned model, which corresponds to an infinite KL-divergence. The plot in Figure 7 depicts the KL-divergence as a function of the sequence length for each of the three settings. Both the table and the plot demonstrate that, in terms of the KL-divergence, our algorithm, which uses odometric information, is robust in the face of data reduction. In contrast, learning without the use of odometry is much more sensitive to reduction in the amount of data.

Again, we applied the two-sample t-test to verify the statistical significance of these results. For example, the KL-divergence being greater for sequences of length 800 than for sequences of length 1000 when learning without the use of odometry is highly statistically significant ($p \ll 0.005$). In contrast, the KL-divergence is not statistically significantly greater when the odometry is used, for either informed or uninformed models. The informed model is even somewhat better, (with moderate statistical significance, $p < 0.11$), when using the sequence of length 800, due to better clustering when there is less accumulated noise on the odometry data.

We note that the data sequence is twice as "wide" when odometry is used than when it is not, that is, there is more information in each element of the sequence when odometry data is recorded. However, the effort of recording this additional odometric information is negligible, and is well rewarded by the fact that fewer observations and less exploration are required for obtaining a data sequence sufficient for adequate learning.

6 Conclusions

Odometric information, which is often readily available, makes it possible to learn HMMs (or POMDP models) for robot navigation efficiently and effectively. If we are interested in learning the geometric relationships between states, using the odometry readings is obviously very helpful. Moreover, our experiments show that even when we are only interested in the underlying topological model, using odometry can both reduce the number of iterations required by the algorithm and improve the resulting model, while requiring shorter data sequences.

The work described in this paper is fairly preliminary. In the very near future, we will extend the example to learn the fully controllable POMDP rather than the HMM. The current implementation uses a very naive clustering algorithm; it will be useful to investigate more sophisticated clustering methods. The algorithm described in this paper is a batch algorithm. It would be useful to adapt it to be an incremental on-line algorithm. Finally, we would like to find an improved M-step that would preserve the additivity constraint.

Acknowledgments

We thank Jim Kurien for providing and supporting the low level code for Ramona, and William Smart and Jason Lango for helping to keep her alive. We are also indebted to John Hughes for the term "additivity" and Sam Trychin for letting us use his skateboard.

This work was supported in part by the Air Force and ARPA under grant No. F30602-95-1-0020, by the NSF in conjunction with ARPA under grant No. IRI-9312395, and by the NSF under grant No. IRI-9453383.

References

[Basye *et al.*, 1995] K. Basye, T. Dean and L. P. Kaelbling. Learning dynamics: System identification for perceptually challenged agents. *Artificial Intelligence*, 72(1), 1995.

[Cassandra *et al.*, 1996] A. R. Cassandra, L. P. Kaelbling and J. A. Kurien. Acting under uncertainty: Discrete Bayesian models for mobile-robot navigation. In *Proceedings of JEEE/RSJ International Conference on Intelligent Robots and Systems*, 1996.

[Cheeseman *et al.*, 1990] P. Cheeseman *et al.* Autoclass: A Bayesian classification system. In J. W. Shavlik and T. G. Dietterich, editors, *Readings in Machine Learning*, pages 296-306. Morgan-Kaufmann, 1990.

[Dempster *et al.*, 1977] A. P. Dempster, N. M. Laird and D. B. Rubin. Maximum likelihood from incomplete data via the EM algorithm. *Journal of the Royal Statistical Society*, 39(1): 1-38, 1977.

[Engelson and McDermott, 1992] S. P. Engelson and D. V. McDermott. Error correction in mobile robot map learning. In *Proceedings of the IEEE International Conference on Robotics and Automation*, pages 2555-2560, Nice, France, May 1992.

[Juang *et al.*, 1986] B. H. Juang, S. E. Levinson and M. M. Sondhi. Maximum likelihood estimation for multivariate mixture observations of Markov chains. *IEEE Transactions on Information Theory*, 32(2), March 1986.

[Juang, 1985] B. H. Juang. Maximum likelihood estimation for mixture multivariate stochastic observations of Markov chains. *AT&T Technical Journal*, 64(6), July-August 1985.

[Koenig and Simmons, 1996a] S. Koenig and R. G. Simmons. Passive distance learning for robot navigation. In *Proceedings of the Thirteenth International Conference on Machine Learning*, pages 266-274, 1996.

[Koenig and Simmons, 1996b] S. Koenig and R. G. Simmons. Unsupervised learning of probabilistic models for robot navigation. In *Proceedings of the IEEE International Conference on Robotics and Automation*, 1996.

[Kuipers and Byun, 1991] B. Kuipers and Y.-T. Byun. A robot exploration and mapping strategy based on a semantic hierarchy of spatial representations. *Journal of Robotics and Autonomous Systems*, 8:47-63, 1991.

[Kullback and Leibler, 1951] S. Kullback and R. A. Leibler. On information and sufficiency. *Annals of Mathematical Statistics*, 22(1):79-86, 1951.

[Liporace, 1982] L. A. Liporace. Maximum likelihood estimation for multivariate observations of Markov sources. *IEEE Transactions on Information Theory*, 28(5), 1982.

[Nourbakhsh *et al.*, 1995] I. Nourbakhsh, R. Powers and S. Birchfield. Dervish: An office-navigating robot. *AI Magazine*, 16(1):53-60, 1995.

[Pierce and Kuipers, 1997] D. Pierce and B. Kuipers. Map learning with uninterpreted sensors and effectors. *Artificial Intelligence*, 1997. (To appear).

[Rabiner, 1989] L. R. Rabiner. A tutorial on hidden Markov models and selected applications in speech recognition. *Proceedings of the IEEE*, 77(2):257-285, February 1989.

[Shatkey and Kaelbling, 1997] H. Shatkey and L. P. Kaelbling. Learning hidden Markov models with geometric information. Technical Report CS-97-04, Department of Computer Science, Brown University, April 1997.

[Simmons and Koenig, 1995] R. G. Simmons and S. Koenig. Probabilistic navigation in partially observable environments. In *Proceedings of the International Joint Conference on Artificial Intelligence*, 1995.

[Thrun and Biicken, 1996a] S. Thrun and A. Biicken. Integrating grid-based and topological maps for mobile robot navigation. In *Proceedings of the Thirteenth National Conference on Artificial Intelligence*, pages 944-950, 1996.

[Thrun and Biicken, 1996b] S. Thrun and A. Biicken. Learning maps for indoor mobile robot navigation. Technical Report CMU-CS-96-121, School of Computer Science, Carnegie Mellon University, Pittsburgh, PA, April 1996.

LEARNING

Learning 8